ce/papers Proceedings in civil engineering

Ernst & Sohn A Wiley Brand

ORIGINAL ARTICLE

eurosteel AMSTERDAM 2023

Ernst & Sohn A Wiley Brand

Experimental investigations of residual stresses in thick high-strength steel plates

Michael Schäfers[1] | Eckehard Müller[2,3]| Martin Mensinger[1]

Correspondence

Michael Schäfers, M.Sc.
Chair of Metal Structures
Technical University of Munich
Email: m.schaefers@tum.de

[1] Chair of Metal Structures, Technical University of Munich, Germany
[2] Laboratory of Applied Physics, University of Applied Sciences, Bochum, Germany
[3] Steinbeis-Transfercenter of Spring Technologies, Component Behavior and Process, Germany

Abstract

Residual stresses strongly influence the load-bearing capacity of steel members under compressive axial loads. Current developments in steel and steel-concrete composite structures imply the use of high-strength steel grades up to 960 MPa. For such steel plates, only limited results of residual stress investigations are known so far. The authors have applied two established measuring methodologies like the sectioning method and X-ray diffraction to determine the residual stress state of 40 mm thick steel plates and different widths. The results show that the distribution and amount of longitudinal residual stresses are mainly determined by the oxyfuel-cutting procedure used to manufacture the specimens. The distribution over the thickness could be determined by X-ray diffraction. Compared to the results of examinations on lower-grade steel plates an assumed correlation of residual stresses and steel grades could not be observed. Consequently, residual stresses have a reduced influence on the load-bearing capacities of structures prone to buckling as the ratio of yield strength to residual stress states declines significantly.

Keywords

residual stresses, high-strength steel, steel plates, sectioning method, X-ray diffraction

1 Introduction

Residual stresses are an important part of steel construction research and have always been subject of discussion. Previous studies have mainly focused on residual stresses in rolled sections. Some studies have been conducted on high-strength steels [1]-[3].

However, only a few studies have been carried out on metal plates (see [4]-[7]). These studies dealt with normal-strength steel grades such as S235 and S355. Here it is shown that the thermal cutting process induces residual stresses for which an idealized approach was derived [8], Figure 1. The compressive residual stresses at the cut edge are assumed to be the magnitude of the yield strength. Further investigations imply that the magnitude of the residual stresses of high-strength steel plates does not correlate to the yield strength [1-3].

This article examines the residual stresses of thermomechanical rolled steel plates with a yield strength of 960 MPa (S960QL, material No. 1.8933) and a thickness of 40 mm. To the best of the authors' knowledge, this configuration of steel grade and plate thickness has not been investigated yet.

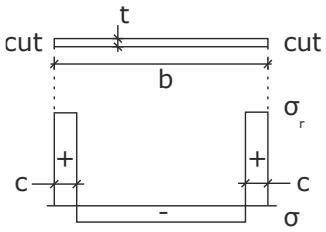

Figure 1 Residual stress distribution of flame cut plates (after [8])

The investigations were made within a research project about steel plates as core section of a novel design of composite columns. The dimensions used in the research project are investigated in this analysis. In this specific case, the cut plates are exposed to normal forces in plane. Thus, longitudinal residual stresses are of high interest. Different manufacturing processes of the plates exist for the newly designed columns, so possible differences between shot-peened and raw plates are to be determined.

https://doi.org/10.1002/cepa.2369

2 Experimental Methods

2.1 Material properties

With increasing steel plates thickness, yield strengths might differ throughout the thickness. Therefore, it can be necessary to evaluate the tensile behaviour of the material on different heights over the section. Experimental Young's moduli can be used later to determine the residual stresses. For plated products, German standard DIN 50125 [9] recommends flat tensile coupons. The ultimate load for such a proportional tensile coupon by far exceeds the maximum loads of common tensile machines. Therefore, it is acceptable to use round tensile coupons with ¼ of the material's thickness according to EN 10025-2 [10].

2.2 Sectioning method

Several destructive and non-destructive methods exist to investigate different local distributions of residual stresses. The sectioning method has become an established procedure to examine longitudinal residual stresses. The background of the procedure is based on the relaxation of steel segments, induced by pre-existing residual stresses and released by partially cutting a specimen into smaller, longitudinally directed segments.

The procedure has been applied in numerous investigations. First, a specimen is prepared with measuring marks which are drilled into the specimen. The distance of the marks should be adapted to the chosen laboratory equipment and the expected gradients of longitudinal residual stresses. Second, the distance between the marks is measured and defined as the reference distance. Measurements are executed on the top and the bottom surface of the specimen. For reliable measurements, a deformeter is considered an appropriate appliance. After measurement, the segments are cut to liberate the internally balanced stress state. Subsequently, strains occur and reveal the inner deformation. This deformation is measured again by the chosen appliance. The measured differences of the lengths can be calculated as strains, related to the initial length, see equation (1). Supposing residual stresses do not exceed the yield strength of the material, Hooke's law can be used to determine the stress from measured strain. Following Bernoulli's assumption of plane sections remaining plane, the resulting strain is averaged from the measurements at the top and bottom of the specimen, see equation (2). It is preferable to use the experimental results of Young's moduli to calculate the residual stresses. In case of strong curvatures of the specimen, the measured distance after the cut (L_f) might not be accurately determined. In specimens close to the fire-cut edges strong bending could be observed. A correctional term needs to be applied to calculate the arclength instead of the length of the chord considering the sagitta of the deformed shape (equation (3)). Corrections only have an effect for a sagitta to measurement length of greater than 0.01. Otherwise, the standard error of measuring precision is greater than the correction term. As the sectioning method is mainly based on the precision it is executed with as well as the experience of the user, it needs to be carried out with all due care. It is recommended to repeat each measurement at least three times and averaging it ($\bar{L}_f$). If measurements deviate more than 0.015 mm from each other, the whole procedure must be repeated, for deviations less than 0.015 and higher than 0.01 mm two measurements are to be carried out additionally.

$$\varepsilon_0 = \left[\frac{\bar{L}_i - \bar{L}_f}{\bar{L}}\right]_{\text{specimen}} \qquad (1)$$

$$\sigma = -E \cdot \frac{\varepsilon_{top} + \varepsilon_{bottom}}{2} \qquad (2)$$

$$\bar{\varepsilon} = \varepsilon_0 + \frac{\left(\frac{\delta}{L}\right)^2}{6\left(\frac{\delta}{L}\right)^4 + 1} \qquad (3)$$

$\frac{\delta}{L}$ relation of sagitta to measurement length

2.3 X-ray diffraction method

Non-destructive methods include the neutron diffraction method or X-ray diffraction to expose residual stress states in layers. These procedures allow a higher resolution of the local stress distribution and constitute a suitable supplementary investigation to the global and lower resolved sectioning method. As a convenient and flexible method, X-ray diffraction has become state-of-the-art. The principle of this procedure is based on irradiating the material with incident X-rays and the rays are reflected at the different atomic layers.

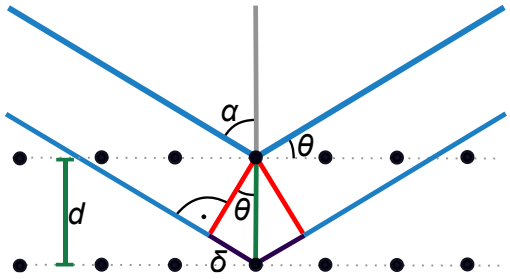

Figure 2 Principle of Bragg reflection

Under Braggs law (4), a maximum intensity of the reflected X-rays is obtained under the angle θ [11] if the following equation is fulfilled:

$$2 \cdot d \cdot \sin\theta = \lambda \qquad (4)$$

with d the lattice spacing, λ the wavelength of the X-rays (see Figure 2). To evaluate the strains, the cos-α-method can be used where the reflected X-rays fulfilling equation (1) give (for polycrystalline materials) a ring, the so-called Debye-Scherrer ring. The shift of this ring is linear to the cosine of circumferential angle α, and the amount of this shift shows the actual strain. This corresponds to the macroscopic strain that is proportional to the microscopic strain. With the help of the Young's modulus and Poisson's ratio, the stress can be calculated. The error of a single measurement is up to ± 30 MPa. To obtain a residual stress profile over the depth, the above material must be removed electrolytically to induce no further stresses.

3 Experimental procedure

3.1 Tensile coupons

For the investigations in this study, thermomechanical hot rolled structural steel with yield strength of 960 MPa (S960QL) with 40 mm thickness was used. Miniature tensile specimens were taken from two heights of the steel plate, at mid-height and a quarter of the thickness. Proportional round tensile coupons according to DIN 50125-A12 [9] with diameter of 10 mm were milled (Figure 3).

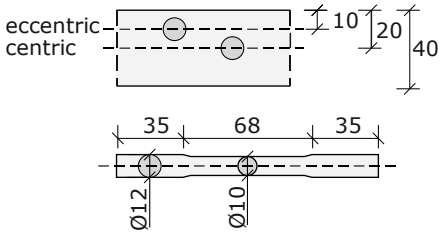

Figure 3 Tensile test position and geometry according to DIN 50125-A12, dimensions in [mm]

Results (given in Table 1) showed no significant difference between centric and eccentric probes for yield strength $R_{p0,2}$, tensile strength R_m, and elongation at rupture A. Only the Youngs' moduli show some deviation, originating from larger standard deviations of the individual tests.

Table 1 Result from tensile tests S960QL

Tensile test position (n=3)	$R_{p0,2}$ [MPa]	R_m [MPa]	Young's modulus [GPa]	A [%]
centric	1003	1073	205.205	16.4
eccentric	1004	1075	215.929	16.4

3.2 Experimental sectioning

For the sectioning method, three specimens were flame cut from plates using oxyfuel cutting. The dimensions of plate 1 and plate 2 are chosen equivalent as used in the further research project about composite columns. Plate 3 was designed double the width of plate 1 and 2 (width = 300 mm, see Figure 4). After cutting the specimens, plate 1 and 3 were shot peened with round grain, reaching a surface roughness of Sa 2 ½. Plate 2 was not treated after cut, so rolling skin and scale were still present.

At its ends, each specimen was cut transverse to its length. To minimize the transverse influence of the heat-affected zone, it is recommended to ensure a total length of at least three times the specimen's width [12]. Thus, buffering zones with lengths of 1.5 to 2 times the width result at the plates ends, and the measuring segments are free of transverse interferences. Following the flame cutting process, single test segments are prepared. Single segments of 300 mm lengths are marked onto the specimens. The width of each segment is recommended in the literature [5] and should be chosen as small as possible for areas of high stress gradients. However, the width should not be taken too narrow, securing an executable cutting procedure with respect to cutting tolerances. For all specimens, a segmental width of 10 mm was chosen. Thus, for each of plates 1 and 2, two specimens with 15 segments can be prepared. For the wider specimen plate 3, two times thirty segments result. The measuring length for the segments was determined by the utilized measurement device, a deformeter with a measuring range of ±50 mm at a total gauge length of 250 mm (Figure 5). The digital dial gauge shows values with a calibrated accuracy of ±0.01 mm. The segment's length was chosen 50 mm longer than the actual measuring length to eliminate the local effects of transverse sawing.

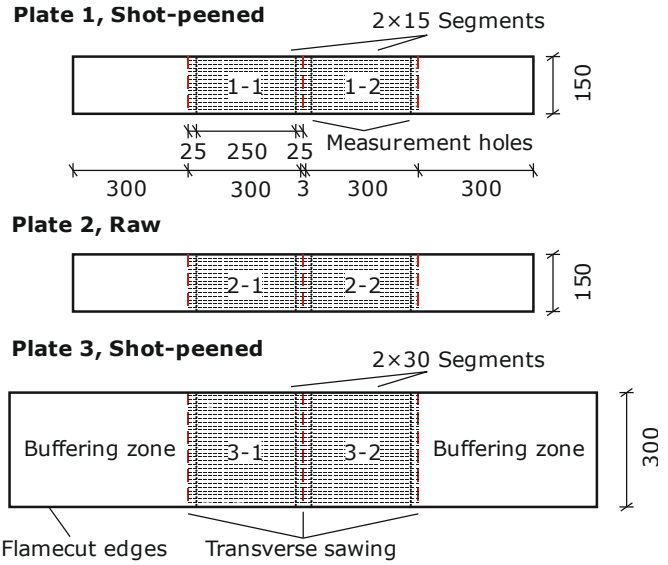

Figure 4 Dimensions of the specimens for the sectioning method, dimensions in [mm]

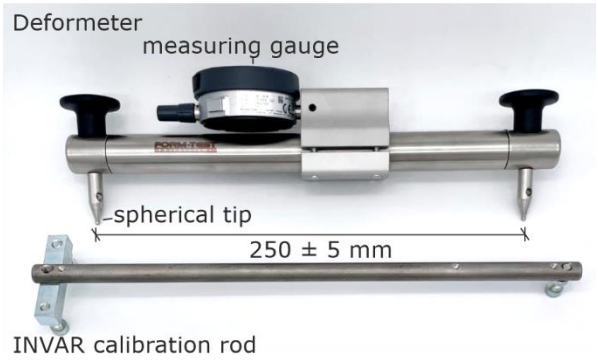

Figure 5 Deformeter with INVAR calibration rod

On top and bottom of each potential segment, the position of the measuring distance is marked, and holes are provided using a center drill (Figure 7). These holes should all be prepared similarly with an appropriate depth and afterwards be cleaned from drilling chips using compressed air. At the ends of the deformeter, there are two spherical measuring tips that should not slip out of the previously drilled holes during measurements (Figure 6 a).

Figure 6 Steps of the sectioning method a) measuring initial distances, b) band sawing c) water jet cutting the segments.

After that, the test segments with the prepared measurement holes were separated with a band saw. However, it quickly became apparent that due to the high strength of the material no sufficient dimensional accuracy of the cuts could be ensured. In addition, extreme wear could be found on the used saw bands. The feed rate was greatly reduced, but despite a constant supply of coolant, a thermal effect of the saw cut, could not be ruled out. Since the process reliability of the cut was subsequently no longer given, the cutting process had to be changed. An abrasive waterjet cutting machine was used (Figure 6 c). The advantages of using waterjet cutting are manifold, such as a much higher precision of each cut. Furthermore, due to the surrounding water basin, the heat input into the material remains low and prevailing stress states remain unaffected. Furthermore, the wear due to the separation process of high-strength material is reduced. Immediately after cutting, the components had to be removed from the cutting basin and had to be dried with compressed air to avoid corrosion in the measuring holes. The disadvantages of water jet cutting are high cost and slow rate of progress. In this case, they are outweighed by the advantages.

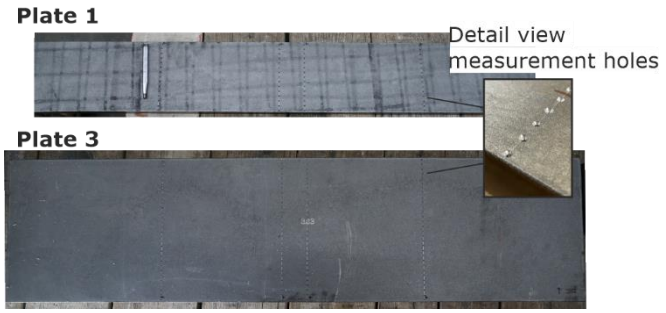

Figure 7 Prepared specimens with detail view of measurement holes

The obtained segments were measured using the deformeter prior to and after cutting. The deviation of the measurement distance was determined, whereas the gauge length was calibrated with the help of an INVAR rod. Each measurement was directly transmitted from the dial gauge into a measuring computer by a signaling cable and was repeated three times. After cutting the segments, the measurements of the distances were repeated. Both measurements, before and after cutting, were carried out at room temperature with a difference of ± 2°C to avoid length expansion due to temperature difference. With this sequence, possible influences on the specimen's temperature due to the cutting process are excluded.

In the outermost segments near the oxyfuel cutting edges, strong bending was observed after separation. The sagitta of the curvature was determined with the help of a special measuring instrument (see Figure 8). Due to the irregularities and tolerances of the waterjet cutting, the width of each segment was different, and a small number of segments were even unusable because of destruction of the measurement holes. For some segments, the width of each cut differed due to irregularities and tolerances from the waterjet cutting. A small number of segments could not be measured finally as the water jet cutting destroyed the measurement holes.

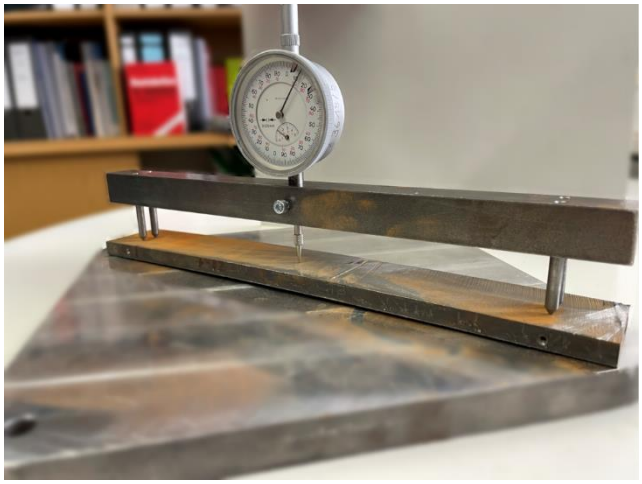

Figure 8 Sagitta measurement of curved segment on planar surface

3.3 X-ray diffraction

The cut segments of the sectioning method were used for further investigations. In a first step, three specimens from the prior waterjet cutting have been selected. Two segments were chosen from the inner part of specimens 1-2 and 2-1 (ending -7), one segment was chosen as the outermost of specimen 1-2 (-15), as seen in Figure 9 a. For these specimens, X-ray diffraction was executed in steps of 50 µm from top and bottom (Figure 9 b) using acid to expose the underlying lattice. To receive a distribution over height, specimen 2-1-7 was further examined on the cut edge. For all measurements, the cos-α-method was used [13, 14].

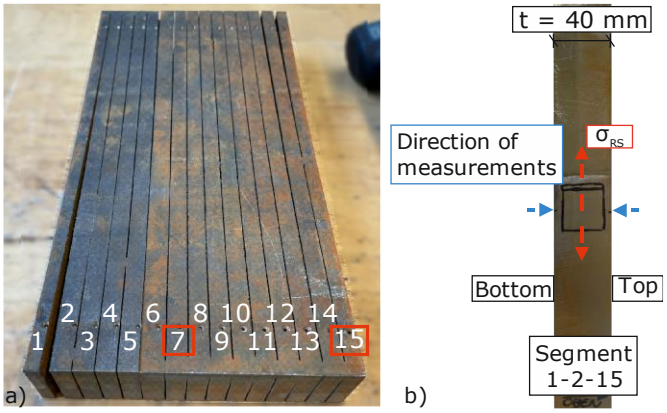

Figure 9 Direction of X-ray diffraction for measurements from top and bottom for prior cut segments

4 Results

The mean residual stresses of all narrow specimens (1-1, 1-2, 2-1 and 2-2) and the wider specimens (3-1 and 3-2) show tensile stresses of around 150-200 MPa in the lateral segments near the cutting edges (Figure 10). These can be localized only in the outer segments; all other segments have revealed compressive stresses of around 0 to 60 MPa. Overall, it is noticeable that the measurement shows high scattering. The sum of all measurements ("I", legend Figure 10) should ideally be zero and can be regarded as measurement accuracy. Deviations lead to an overweight of the compressive stresses in the specimens and can be explained by the limited measurement precision that results in a possible accuracy of at least ± 8 MPa for each segment. Furthermore, the width of 10 mm might not be sufficiently narrow to record strains in areas of high gradients, as in the lateral segments. Calculations in [8] imply a width of the area under tensile stresses of 7.25 mm for the chosen geometry. Further, it can be stated that no significant influence could be observed by the initial width of the specimens and the distribution can be well approximated by established approaches (Figure 1). Also, no significant difference of the longitudinal residual stresses was observed between plate 1 and plate 2, resulting from the shot peening.

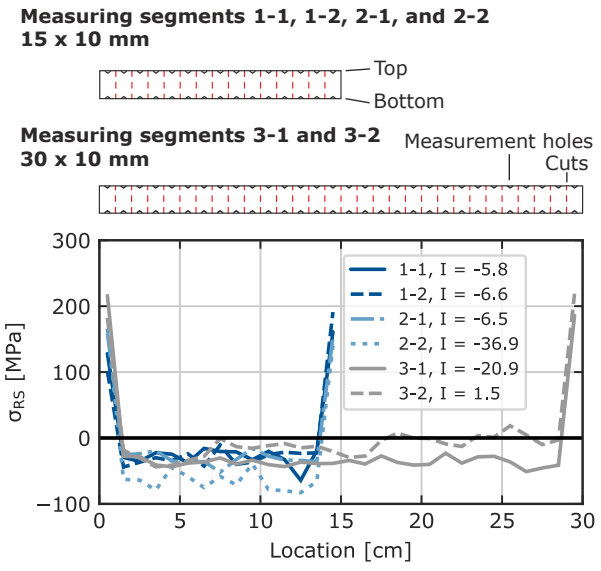

Figure 10 Results of the sectioning method

Using X-ray diffraction methods, it is possible to reduce the spacing of measurements and monitor local distributions of residual stresses closely over the specimen's thickness. The measurements were carried out on cut samples from the sectioning method where longitudinal stresses are expected to have been degraded. On the cutting surface of segment 2-1-7, the stress distribution over the thickness of the plate (t = 40 mm, Figure 9 b) was determined. As to be seen in Figure 11, compressive stresses occur of around -100 MPa close to the edges. These change to tensile stresses within a depth of around 7.5 mm.

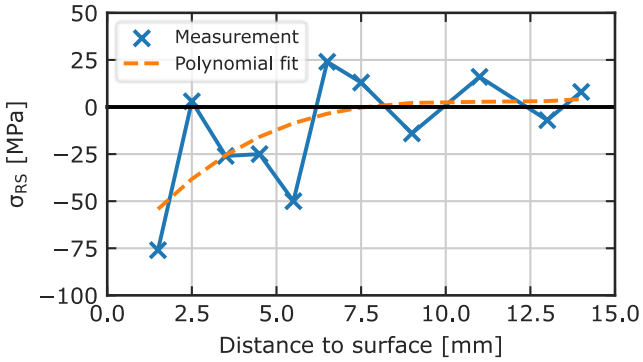

Figure 11 Residual stress distribution over height (Segment 2-1-7)

Further measurements with higher spatial resolution were executed on the top and bottom surfaces of three segments. This enabled quantifying the influence of the follow-up treatment, the shot peening. From plastic deformations due to the shot peening, elevated compressive residual stresses with a peak value of -500 MPa establish up to a depth of 400-500 µm before they lead to zero (Figure 12). The raw specimen (2-1-7) shows constant compressive residual stresses on the top and bottom of around -100 MPa, corresponding to the measurement on the cutting surface. Integration of the compressive stresses leads to a resulting tensile stress of around 16 MPa in the inner part of the segment.

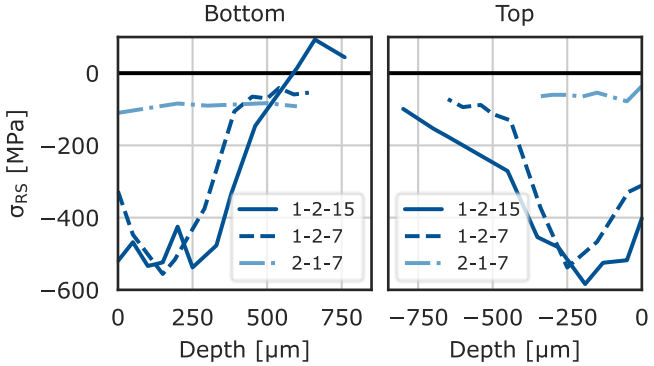

Figure 12 Residual stresses near surface (Segments 1-2-15, 1-2-7 and 2-1-7)

5 Conclusion

Experimental investigations of residual stresses on flame-cut high-strength metal plates (S960QL) were presented. The sectioning method as a destructive and the X-ray diffraction method as a non-destructive method was used. The results of both methods show high scattering.

In the determined results, an influence of the plate width could hardly be determined during the investigation. The influence of the heat-affected zone due to flame cutting influences the global residual stress in the rolling direction significantly. The results seem comparable to examinations at lower steel grades in magnitude and distribution. Post-treatment by shot peening showed no influence on the global longitudinal residual stress state. This means high agreement with results from the literature in investigations of plates with normal-strength steels. The prevailing residual stresses can thus be scaled as imperfections to the yield strength of the base material. Due to the greatly increased yield strength of S960QL, the influence of residual stresses is significantly reduced. It can therefore be assumed that there is less structural imperfection which leads to less influence on the load-bearing behavior of components that are at risk of stability.

The selected measurement procedures are considered established methods for the investigation of residual stresses. The use of the sectioning method is no longer necessarily up-to-date and should be questioned due to the time-consuming separation process, the systematically inaccurate measurements obtained with manual measuring equipment and its high reliance on the user's experience. At this point, the use of strain gauges in combination with precise waterjet cutting would be favorable, whereby strain can be measured with great accuracy. Complete cutting is also not necessary, which further reduces the scope of the cutting work. On the other hand, the X-ray diffraction method presented reliable measurements with comparably little effort. Residual stresses can be examined at a high resolution. In future, this procedure can extensively be used because newly developed equipment is portable and can measure whole components.

Acknowledgement

All investigations were done as part of the research project "Composite columns with laminated hight-strength steel plates for building construction". The IGF-project 21366 N of the Research Association for Steel Application (FOSTA e.V.) is a sub-project of the FOSTA-research cluster "HOCHFEST" and is funded by the AiF within the program of Industrial Collective Research (IGF) from the Federal Ministry for Economic Affairs and Climate Action of Germany on the basis of a decision made by the German Bundestag. Special appreciation to the workshop of the Institute of Plant and Process Technology at the Technical University of Munich for executing the water jet cutting.

References

[1] Ban, H.; Shi, G.; Shi, Y. et al. (2012) Residual Stress Tests of High-Strength Steel Equal Angles. In: Journal of Structural Engineering 138, Vol. 12, pp. 1446-1454.

[2] Ban, H.; Shi, G.; Bai, Y. et al. (2013) Residual stress of 460 MPa high strength steel welded I section: Experimental investigation and modeling. In: International Journal of Steel Structures 13, Vol. 4, pp. 691-705.

[3] Shi, G.; Hu, F.; Shi, Y. (2014) Recent research advances of high strength steel structures and codification of design specification in China. In: International Journal of Steel Structures 14 Vol. 4, pp. 873-887.

[4] Tebedge, N.; Alpsten, G. A.; Tall, L. (1971) Measurement of residual stresses - a study of methods.

[5] Tebedge, N.; Alpsten, G.; Tall, L. (1973) Residual-stress measurement by the sectioning method. In: Experimental Mechanics 13 Vol. 2, pp. 88-96.

[6] Young, B.W.; Dwight, J.B. (1971) Residual stresses and their effects on the moment-curvature properties of structural steel sections, CIRIA Tech. Note 32

[7] Thiébaud, R.; Lebet, J.-P. (2012) Experimental study of residual stresses in thick steel plates. In: *SSRC Annual Stability Conference Proceedings*, Grapevine, Texas, USA.

[8] European Convention for Constructional Steelwork (1976) Manual on stability of steel structures

[9] German standard DIN 50125:2022-08, Testing of metallic materials - Tensile test pieces.

[10] EN 10025-2:2019-10, Hot rolled products of structural steels - Part 2: Technical delivery conditions for non-alloy structural steels.

[11] Kittel, Ch (2018) Kittel's Introduction to Solid State Physics. 9. edition, Wiley, Hoboken,

[12] Huber, A. W.; Beedle, L. S. (1954) Residual stress and the compressive strength of steel, Welding Journal, Vol. 33, No. 12.

[13] Tanaka, K., Akiniwa, Y. (2004) Diffraction Measurements of Residual Macrostress and Microstress Using X-Rays, Synchrotron and Neutrons, JSME International Journal Series A, 47, pp. 252- 263.

[14] Sasaki, T. Mizuno, R., Takago, S., Mishima, Y. (2021) Standardization of Cosα Method for X-Ray Stress Measurement, Materials Science Forum, Vol. 1016, pp.1240-1245